Acta Crystallographica Section D
Biological Crystallography
ISSN 0907-4449

Binding of *N*-acetylglucosamine to chicken egg lysozyme: a powder diffraction study

R. B. Von Dreele

Manuel Lujan Jr Neutron Scattering Center, MS H805, Los Alamos National Laboratory, Los Alamos, NM 87545, USA

Correspondence e-mail: vondreele@lanl.gov

Received 6 July 2001
Accepted 25 September 2001

PDB References: Lysozyme, buffer pH 5.0, 1ja2; NAG–lysozyme, buffer pH 5.0, 1ja4; Lysozyme, buffer pH 6.0, 1ja6; NAG–lysozyme, buffer pH 6.0, 1ja7.

The binding of *N*-acetylglucosamine (NAG) to chicken egg lysozyme (E.C. 3.2.1.17) was investigated by high-resolution X-ray powder diffraction at room temperature. NAG was found to bind to lysozyme in a rapid precipitation preparation with 0.05 *M* NaCl buffer pH 6.0, but not 0.05 *M* NaCl buffer pH 5.0. Binding was indicated by significant and readily apparent changes in the diffraction pattern from that of the apo protein precipitated from the same solvent. The location of NAG bound to lysozyme was easily found from a difference Fourier map generated from structure factors extracted during a preliminary combined Rietveld and stereochemical restraint refinement. Full protein and protein–NAG structures were refined with these techniques (R_{wp} = 2.22–2.49%, R_p = 1.79–1.95%, R_F^2 = 4.95–6.35%) and revealed a binding mode for NAG which differed from that found in an earlier single-crystal study and probably represents a precursor trapped by rapid precipitation.

1. Introduction

With the decoding of the human and other genomes (Aldhous, 2000; Pennisi, 2000; Venter *et al.*, 2001; International Human Genome Sequencing Consortium, 2001), the paradigm of drug discovery will change to one that is focused on molecular design for interaction with specific proteins. This new emphasis on proteomics will require experimental verification of the details of protein–ligand interactions under a wide variety of conditions. Current techniques either require formation of single crystals of the protein–ligand complex of sufficient quality for X-ray diffraction work or else interpretation of NMR spectra. This work is difficult, as indicated by a cursory examination of the Protein Data Bank which shows only about 10% of the entries involve protein–ligand complexes. For the case considered here, after early crystallographic studies of chicken egg lysozyme (E.C. 3.2.1.17; Blake *et al.*, 1962, 1965; Phillips, 1967) work immediately focused on the binding of mono- and oligosaccharides of *N*-acetylglucosamine (NAG) to this protein (Johnson & Phillips, 1965; Blake *et al.*, 1967; Perkins *et al.*, 1978; Cheetham *et al.*, 1992) to understand the molecular basis of the enzymatic cleavage of these materials and similar mucopolysaccharide components of bacterial cell walls (Rupley & Gates, 1967). For the NAG–lysozyme complex, single crystals were typically soaked for 24 h (Perkins *et al.*, 1978). Cracking of the crystals was frequently observed and could be controlled only by careful selection of concentrations and pH. The soaking time and conditions were sufficient to allow α/β-NAG interconversion, so that both anomers were found in this structure. Single crystals of the tri-*N*-acetylchitotriose (NAG_3) complex

with lysozyme (Cheetham *et al.*, 1992) were grown by cocrystallization; the highest quality crystals were obtained only after three weeks crystal growth starting from a 1:1 stoichiometric mixture. This period was sufficiently long that the inhibitor was partially hydrolyzed by the enzyme; consequently, the final structural result showed only 55% occupancy in the binding site. In both cases, small but discernable changes in the tetragonal lysozyme lattice parameters were evident upon formation of the complex. For NAG–lysozyme a = 78.4, c = 38.3 Å and for NAG_3–lysozyme a = 78.86, c = 38.25 Å, compared with the apo-protein where a = 79.2, c = 38.0 Å (Perkins *et al.*, 1978; Cheetham *et al.*, 1992). NMR studies (Perkins *et al.*, 1981) tended to confirm the crystallographic results for binding of NAG, but suggested that possible alternative binding sites also existed in solution. The results of these studies showed that there are six possible binding sites (*A*–*F*) across the cleft in the protein surface and that all could be occupied by a sequence of six units in a polyacetoamidosaccharide. In NAG_3–lysozyme three of these sites (*A*–*C*) are occupied and the two α/β-anomers of NAG were found in two different locations about the *C* site (Blake *et al.*, 1967; Perkins *et al.*, 1978; Cheetham *et al.*, 1992). Based on this crystallographic work and chemical studies of the enzymatic activity of lysozyme (Rupley & Gates, 1967), the catalytic site was located between the *C* and *D* binding sites and involves residues Glu35 and Asp52. The binding of NAG in either anomer form in the *C* site gives a rationale for it acting as an inhibitor, as it prevents binding of an oligosaccharide across the catalytic site. Interestingly, the crystallographic binding site found for NAG_3 is not the catalytically effective one so this material is a self-inhibitor.

Table 1
Crystallographic and refinement data for *N*-acetyl-D-glucosamine–lysozyme complexes.

NAG = *N*-acetylglucosamine. Values in parentheses are estimated standard deviations in the values shown. pH measurements were taken with a LAZAR Research Laboratories PHR-146 Micro Combination electrode calibrated with pH 4.00 and pH 7.00 standard buffers (Fisher Sci.). Wavelength calibrations were obtained from the fitted positions of six reflections from an NIST SRM1976 alumina plate. Data-collection step count times were determined by the following algorithm: for $2\theta < 5^\circ$, $t = 4$ s; for $2\theta > 5^\circ$, $t = 6.4691 - 0.9877(2\theta) + 0.0988(2\theta)^2$ s. The residuals $R_{wp} = 100[\sum w(I_o - I_c)^2/\sum wI_o^2]^{1/2}$, $R_p = 100\sum |I_o - I_c|/\sum I_o$ and $R_F^2 = 100\sum |F_o^2 - F_c^2|/\sum F_o^2$, where I_o and I_c are the observed and calculated powder diffraction profile intensities and w is the weight associated with I_o. F_o^2 is the value of the structure factor extracted during the Rietveld refinement and F_c^2 is the calculated structure factor. *PROCHECK* (Laskowski *et al.*, 1993) compares protein stereochemistry with expected values (Engh & Huber, 1991; Morris *et al.*, 1992).

Material	Lysozyme	NAG–lysozyme	Lysozyme	NAG–lysozyme
Crystal data				
Space group	$P4_32_12$	$P4_32_12$	$P4_32_12$	$P4_32_12$
a (Å)	79.1317 (11)	78.9631 (10)	78.5689 (15)	78.5240 (14)
c (Å)	38.0297 (10)	38.2151 (10)	38.5134 (15)	38.5731 (14)
V (Å^3)	238135 (8)	238277 (9)	237746 (12)	237842 (12)
PDB code	1ja6	1ja7	1ja2	1ja4
Powder data collection				
Buffer pH	6.00	6.00	5.00	5.00
Measured pH	5.2	5.1	4.8	4.8
λ (Å)	0.699970 (1)	0.699842 (1)	0.700030 (1)	0.700030 (1)
2θ range (°)	1.0–13.580	1.0–13.498	1.0–13.994	1.0–13.698
$\Delta 2\theta$ (°)	0.002	0.002	0.002	0.002
N_{steps}	6291	6250	6497	6350
Step time (s)	4.0–11.25	4.0–11.13	4.0–12.04	4.0–11.51
Combined Rietveld and stereochemical restraint refinement results				
N_{ref}	2824	2758	3112	2874
Resolution (Å)	40.11–2.96	40.10–2.98	40.03–2.87	40.11–2.94
$N_{restraints}$	5019	5091	5073	5028
$N_{obs} = N_{restraints} + N_{steps}$	11310	11341	11570	11378
$N_{parameters}$	3025	3069	3025	3023
R_{wp} (%)	2.49	2.48	2.22	2.28
R_p (%)	1.95	1.94	1.79	1.81
R_F^2 (%)	6.09	4.95	5.32	6.35
Powder profile parameters				
X	0.019 (12)	0.084 (11)	0.453 (14)	0.347 (14)
X_e	0.112 (21)	0.117 (21)	0.499 (25)	0.262 (25)
Y	1.36 (28)	0	0	0
Y_e	0.3 (5)	4.7 (5)	0	0
Protein chain parameters from *PROCHECK*				
Bond error (Å)	0.010	0.011	0.011	0.011
Angle error (°)	1.66	1.71	1.73	1.74
Residues in core region (%)	87.6	85.8	86.7	86.7
ω torsion-angle error (°)	2.8	2.7	2.7	2.6
Bad contacts per 100 residues	3.1	0.8	1.6	0.0
ζ-angle error (°)	1.7	2.0	1.8	1.8
Hydrogen-bond energy error (kJ mol^{-1})	2.9	2.9	4.6	4.1
RMS deviations from planes (Å)	0.005	0.004	0.006	0.006

Recent work (Von Dreele, 1999; Von Dreele *et al.*, 2000) has shown that powder diffraction may be a useful tool for examining protein structures. Powder diffraction patterns can display considerable sensitivity to subtle structural changes *via* shifts in the diffraction peak positions and changes in intensity. This work showed that protein lattice-parameter determinations from powder data are perhaps two orders of magnitude more precise than those obtained from typical single-crystal experiments and that combined Rietveld (1969) and stereochemical restraint refinements can give protein structures of moderate (~3 Å) resolution. For the study of protein–ligand complexes, powder diffraction offers a distinct advantage over single-crystal work in its complete immunity to crystal fracture or even a phase change that may accompany complex formation. Moreover, rapid formation of a polycrystalline precipitate allows possible exploration of initial complex formation under a wide variety of conditions not accessible in slow soaking or single-crystal growth experiments. In this work, we demonstrate the use of high-resolution X-ray powder diffraction for protein–ligand structure determination

in a study of the binding of *N*-acetyglucosamine to chicken egg lysozyme.

2. Experimental

Chicken egg lysozyme (E.C. 3.2.1.17; FisherBiotech, 3× crystallized, lot Nos. 995417-12 and 996924-12) and *N*-acetylglucosamine (NAG; ICN Biomedicals, Inc. lot No. R9745) 0.05 *M* Na_2HPO_4/KH_2PO_4 buffer pH 5.0 (Fisher Sci.), 0.05 *M* potassium hydrogen phthalate/NaOH buffer pH 5.0 (Hydrion, Aldrich Chemical Co.) and NaCl ('Certified for Biological Use', Fisher Sci.) were used as received. In a typical sample preparation, a polycrystalline slurry was made by combining ∼20 mg lysozyme (1.4 µmol), ∼10 mg NAG (45 µmol) and 200 µl 0.5 *M* NaCl buffer pH 6.0 with an agate mortar and pestle. Polycrystalline precipitate formed within a few seconds. The slurry was loaded into a 1.5 mm diameter glass capillary and centrifuged to pack the slurry. Excess mother liquor was removed and the capillary was flame-sealed to prevent subsequent solvent evaporation. In a similar way, a polycrystalline sample of unbound lysozyme in 0.5 *M* NaCl buffer pH 6.0 was prepared. Similar samples with 0.5 *M* NaCl buffer pH 5.0 were also prepared. Samples were ∼8 mm long. As each sample was prepared, high-resolution X-ray powder diffraction data were immediately collected at room temperature (290 K) on beamline X3b1 at the National Synchrotron Light Source, Brookhaven National Laboratory equipped with a double Si(111) monochromator and a Ge(111) analyser; the sample was spun during data collection to ensure good powder averaging. Details of the data collections are given in Table 1.

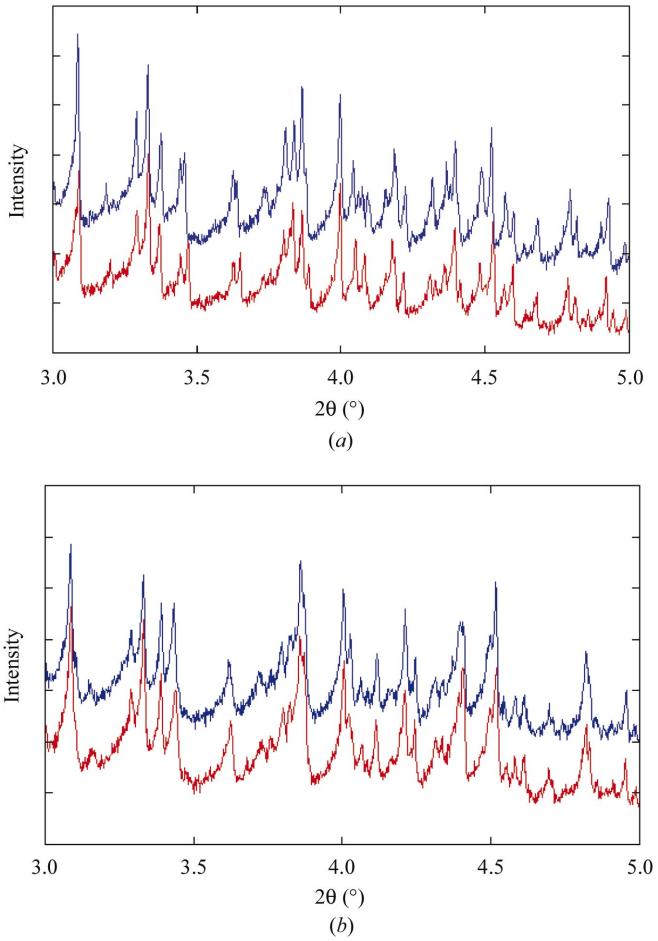

Figure 1
(*a*) A small segment of high-resolution X-ray powder diffraction patterns of lysozyme (red) and lysozyme–*N*-acetylglucosamine mixture (blue) precipated from 0.5 *M* NaCl buffer pH 6.0 taken with λ = 0.70 Å. The latter pattern has been offset for clarity. (*b*) A small segment of high-resolution X-ray powder-diffraction patterns of lysozyme (red) and lysozyme–*N*-acetylglucosamine mixture (blue) precipated from 0.5 *M* NaCl buffer pH 5.0 taken with λ = 0.70 Å. The latter pattern has been offset for clarity.

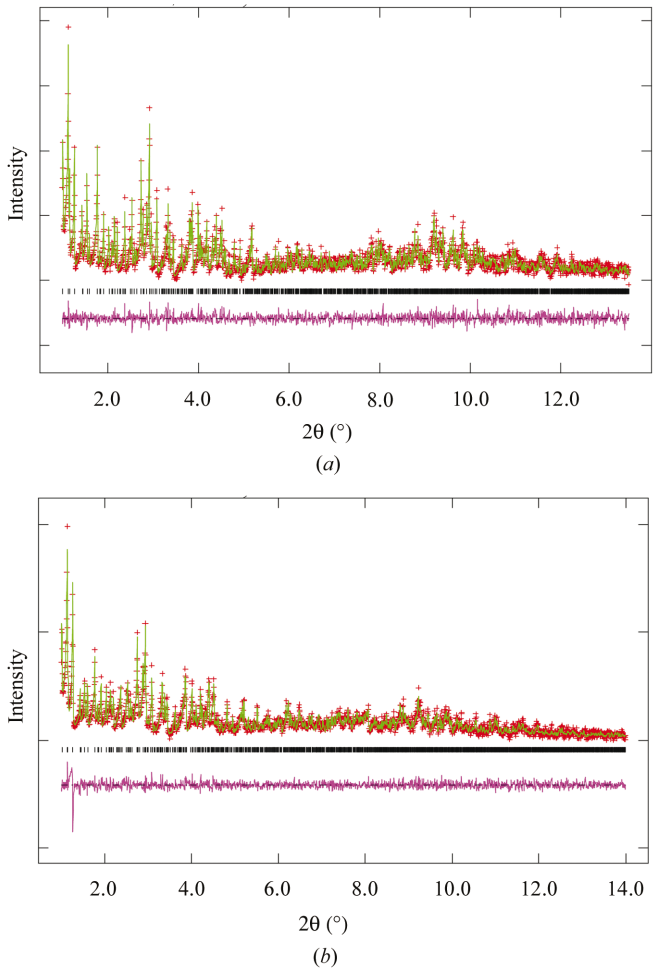

Figure 2
(*a*) High-resolution X-ray powder-diffraction profile from the final Rietveld refinement of lysozyme precipated from 0.5 *M* NaCl buffer pH 6.0. Observed intensities are shown as red +, calculated and difference curves as green and magenta lines and the reflection positions are shown as black |. The background intensity found in the refinement has been subtracted from the observed and calculated intensities for clarity. (*b*). High-resolution X-ray powder diffraction profile from the final Rietveld refinement of lysozyme precipated from 0.5 *M* NaCl buffer pH 5.0. Observed intensities are shown as red +, calculated and difference curves as green and magenta lines and the reflection positions are shown as black |. The background intensity found in the refinement has been subtracted from the observed and calculated intensities for clarity.

Visual comparison of the diffraction patterns obtained from lysozyme and NAG–lysozyme polycrystalline slurries formed in 0.5 *M* NaCl buffer pH 6.0 (Fig. 1*a*) clearly show that a structural modification has occurred associated with the formation of an NAG–lysozyme complex. The patterns show differences in peak positions, which arise from lattice-parameter changes, and differences in intensity associated with the crystal structure modification. There were no changes evident in a comparison of the powder patterns of lysozyme and NAG–lysozyme slurries prepared with 0.5 *M* NaCl buffer pH 5.0 (Fig. 1*b*).

The crystal structures of lysozyme precipitated from the pH 5.0 and pH 6.0 buffers were subject to a combined Rietveld and stereochemical restraint least-squares refinement using techniques described previously (Von Dreele, 1999; Von Dreele *et al.*, 2000) and the General Structure Analysis System (*GSAS*; Larson & Von Dreele, 2000). The starting model for the lysozyme atom coordinates was taken from PDB entry 1rfp (Motoshima *et al.*, 1997). Protein refinement was achieved by constructing a band-diagonal approximation to the full matrix; band-matrix routines from the *SLATEC* suite (Fong *et al.*, 1993) were adapted for use in *GSAS*. A matrix bandwidth of 300 parameters was chosen for refinement of all lysozyme structures studied here. During both sets of Rietveld refinements the resulting protein stereochemistry was periodically evaluated with the *PROCHECK* (Laskowski *et al.*, 1993) suite of programs and graphically examined using the *Swiss-PdbViewer* package (Guex & Peitsch, 1999). Details of these refinements are listed in Table 1 and the resulting fitted powder diffraction profiles are shown in Figs. 2(*a*) and 2(*b*).

The lysozyme structures obtained above were then used as starting models for the analysis of the lysozyme–NAG powder diffraction data. After preliminary combined Rietveld and stereochemical refinements for the materials precipitated from both pH 6.0 (R_{wp} = 2.61%, R_p = 2.04%, R_F^2 = 6.03%) and pH 5.0 (residuals in Table 1) buffers, difference Fourier maps were constructed in each case by using structure factors extracted from the respective powder diffraction profiles. This extraction process operates during the Rietveld refinement by apportioning the observed diffraction profile above background among the contributing reflections according to the ratio of their calculated intensities. In this way, a set of integrated intensities are obtained for all reflections within the range of the powder profile; they are then subjected to the usual corrections for reflection multiplicity, Lorentz and

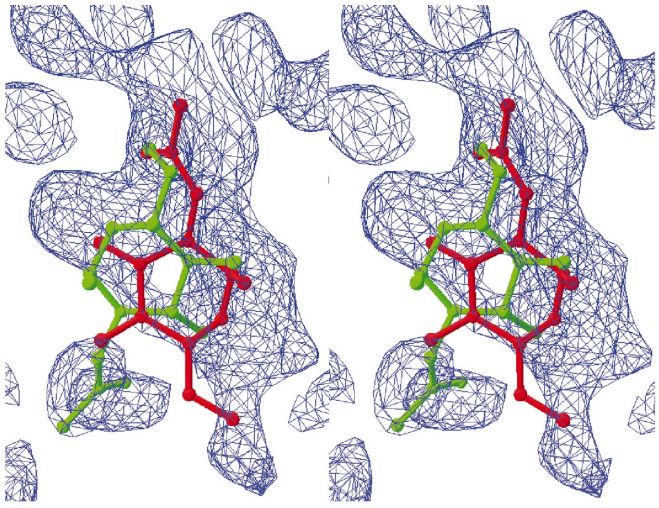

Figure 3
Stereographic representation of the ΔF map at 1.5σ. The map was developed from structure factors extracted during the Rietveld refinement of the lysozyme structure using the diffraction data obtained from the 0.5 *M* NaCl pH 6.0 NAG–lysozyme material. Superimposed are the NAG molecule (shown in red) found by the final Rietveld refinement of the NAG–lysozyme complex and the NAG molecule (shown in green) found by the single-crystal analysis of Perkins *et al.* (1978).

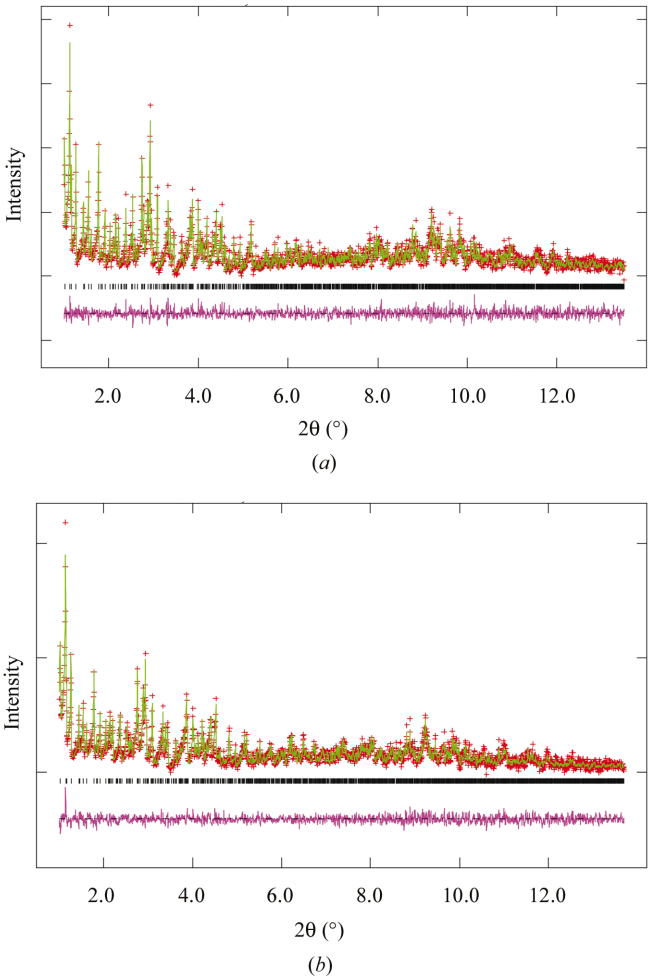

Figure 4
(*a*) High-resolution X-ray powder diffraction profile from the final Rietveld refinement of lysozyme–*N*-acetylglucosamine precipated from 0.5 *M* NaCl buffer pH 6.0. Observed intensities are shown as red +, calculated and difference curves as green and magenta lines and the reflection positions are shown as black |. The background intensity found in the refinement has been subtracted from the observed and calculated intensities for clarity. (*b*) High-resolution X-ray powder diffraction profile from the final Rietveld refinement of lysozyme–*N*-acetylglucosamine precipated from 0.5 *M* NaCl buffer pH 5.0. Observed intensities are shown as red +, calculated and difference curves as green and magenta lines and the reflection positions are shown as black |. The background intensity found in the refinement has been subtracted from the observed and calculated intensities for clarity.

polarization to obtain a set of 'observed' structure factors. The ΔF map (Fig. 3) prepared from these extracted intensities for the material precipitated from pH 6.0 buffer showed an extended region of density only in the vicinity of the previously identified *C* sugar-binding site for lysozyme. In contrast, the ΔF map for the material prepared from pH 5.0 buffer showed only a few scattered peaks in this region.

A model for the lysozyme–NAG complex formed from pH 6.0 buffer was developed by placing a NAG molecule in the α-anomer form to best fit the ΔF map density. After preliminary refinement of the position and orientation of the α-NAG molecule as a rigid body, the entire α-NAG–lysozyme complex was subjected to combined Rietveld and stereochemical refinement. Fig. 3 shows the refined position of the α-NAG molecule relative to the ΔF map density. The results of this refinement are given in Table 1, the resulting fitted powder diffraction profile is shown in Fig. 4 and drawings of the structure are shown in Figs. 5 and 6.

3. Discussion

Our previous high-resolution X-ray powder diffraction studies with metmyoglobin (Von Dreele, 1999) and T_3R_3 Zn insulin complexes (Von Dreele *et al.*, 2000) used samples obtained by grinding previously crystallized protein in its mother liquor and yielded material with extremely sharp diffraction peaks and little or no sample broadening. The apparent crystallite sizes in these cases were on the order of 1 µm and the microstrain broadening effects were less than 0.1%. In the present study, polycrystalline material has been prepared from amorphous lyophilized protein and relatively high-salt buffered solvents. Based on the solubility study of Rosenbaum & Zukoski (1996), the preparation conditions described here are at a lysozyme concentration that exceeds the solubility limit (2.0 mg ml^{-1} at pH 4.7 and 0.5 *M* ionic strength) by about a factor of 50. In all cases, we obtain polycrystalline material that gives extremely sharp diffraction patterns. Interpretation (Larson & Von Dreele, 1986) of the *X*, X_e, *Y* and Y_e coefficients (Table 1) obtained from the Rietveld refinements gives an effective crystallite size of 4–10 µm for the materials prepared from the pH 6.0 buffer and 0.4–1.2 µm for those prepared from the pH 5.0 buffer; the microstrain for both pH 6.0 samples was 0.02–0.08% and no microstrain broadening was observed for the pH 5.0 materials. Evidently, all of the polycrystalline lysozyme samples, prepared here as precipitate, appear to be essentially free of lattice defects and are quite homogeneous, with no variability in lattice parameters. This is in apparent contrast to some reports of differences in single crystals of lysozyme selected from the same solution (Corey *et al.*, 1962; Cheetham *et al.*, 1992).

In the present study, the lattice parameters of lysozyme and α-NAG–lysozyme complex (Table 1) have been determined with unprecedented precision *via* powder diffraction. The precision obtained here approaches one part in 80 000 and is the result of Rietveld refinement fitting of the entire powder-diffraction profile and the extreme sharpness of the peaks; we obtained similar precision in our earlier powder diffraction studies of metmyoglobin and Zn insulin complexes (Von Dreele, 1999; Von Dreele *et al.*, 2000). Consequently, small changes in these values with pH and complex formation are readily apparent and can even be discerned from a simple visual comparison (Figs. 1*a* and 1*b*). The lattice parameters obtained here for lysozyme prepared from 0.5 *M* NaCl buffer pH 6.0 most closely resemble values (*e.g.* a = 79.21, c = 37.97; Motoshima *et al.* 1997) typically given for single crystals obtained from pH 4.7 solutions. Polycrystalline lysozyme prepared from 0.5 *M* NaCl buffer pH 5.0 gave distinctly different lattice parameters with a smaller by 0.71% and c larger by 1.26%. As there is essentially no change in unit-cell volume, it is unlikely that these changes in lattice parameters with pH are a consequence of changes in protein hydration but are more likely to arise from a subtle change in protein conformation. The measured pH values for our preparations are quite close (4.8 and 5.2) so the transition between these two lysozyme structures may be quite sharp. Since single crystals of lysozyme are typically grown at a pH very close to

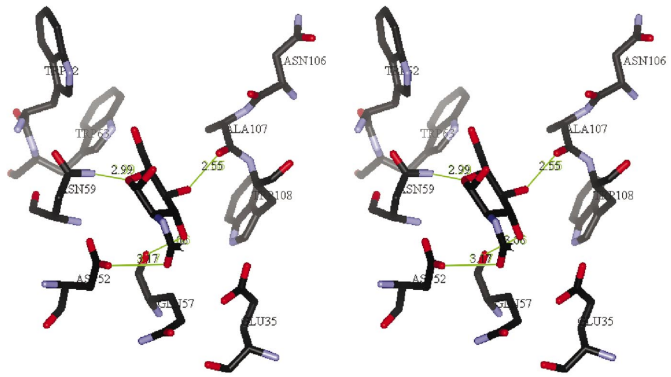

Figure 5
Stereoscopic view of the binding site for *N*-acetylglucosamine on lysozyme. The four possible hydrogen bonds and distances involved in the binding are shown in green.

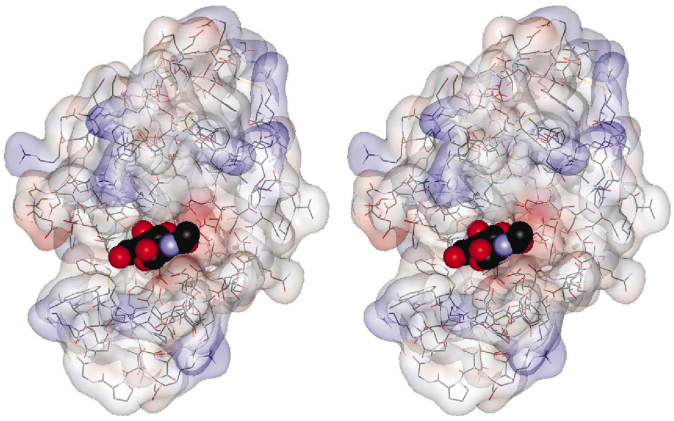

Figure 6
Steroscopic view of molecular surface of lysozyme with a CPK representation of the bound *N*-acetylglucosamine. The protein surface is colored according to the electrostatic potential, where blue is positive and red negative.

this transition, reports of differences in single crystals of lysozyme selected from the same solution (Corey *et al.*, 1962; Cheetham *et al.*, 1992) may have a ready explanation in that some have the higher pH structure while others have the lower pH one.

Formation of the α-NAG–lysozyme complex from 0.5 *M* NaCl pH 6.0 was marked by easily visible changes in the powder diffraction patterns (Fig. 1*a*) and significant changes in the lattice parameters. For the complex, *a* is smaller by 0.21% and *c* larger by 0.49% compared with those of the apo protein precipitated from the same buffer. This change upon complex formation is consistent with the lower precision single-crystal values obtained by Perkins *et al.* (1978) and, interestingly, those obtained by Cheetham *et al.* (1992) for the NAG_3–lysozyme complex. The precipitate from a NAG–lysozyme mixture in 0.5 *M* NaCl pH 5.0 showed no visible change in the powder pattern (Fig. 1*b*) from that of pure lysozyme prepared from the same solvent; the lattice parameters are also essentially unchanged (*a* is smaller by 0.06% and *c* is larger by 0.15%).

The structural orientation of the α-NAG molecule found in this powder diffraction experiment is different from that obtained previously from single-crystal diffraction data (Perkins *et al.*, 1978). Both studies find that the α-NAG molecule occupies the *C* site, but this powder study shows it to be essentially rotated 180° about the sugar-ring axis with respect to the orientation seen in the single-crystal study (*cf.* Fig. 3). Also, in contrast to the single-crystal result, this powder study shows no evidence of any β-NAG in the structure. A number of checks were employed to test the validity of this result. A Rietveld refinement of the site fractions for α-NAG molecules placed in both orientations clearly preferred the powder one (>80%) instead of the single-crystal one (<20%) given by Perkins *et al.* (1978). A similar refinement of the powder site fraction alone for α-NAG indicated essentially 100% occupancy. Moreover, a comparison (Fig. 3) of the two orientations to the ΔF map obtained here shows a much better match for α-NAG in the powder orientation; in particular, the *N*-acetyl group in the single-crystal orientation falls in a relatively low-density region. Consequently, a different pattern of four potential hydrogen bonds (Fig. 5) is used to hold the NAG molecule in the *C* site; these are NAG O3–Gln57 O (3.06 Å), NAG O4–Ala107 O (2.55 Å), NAG O5–Asn59 $N^{\delta2}$ (2.99 Å) and NAG O7–Asp52 $O^{\delta2}$ (3.17 Å). This last interaction may in fact not be a hydrogen bond, as the donor–acceptor distance is rather long and the acidic Asp $C^{\gamma}OOH$ is probably ionized under the pH conditions of the sample (Bonincontro *et al.*, 1998) so no H atom would be available for the bond. Thus, the *N*-acetyl group is not held in its specific binding pocket by the hydrogen bonds NAG N2–Asn59 N and NAG O6–Trp62 $N^{\varepsilon1}$ as seen in the single-crystal study and the structure obtained here (Fig. 6) probably represents a precursor trapped by rapid precipitation. The lack of any β-NAG in this precipitated complex is probably owing to the slow α/β conversion from the α-form present in the solid NAG used to make up this sample; in contrast, the slow soaking procedure used by Perkins *et al.* (1978) ensured that an equilibrium mixture of α/β-NAG was available for complex formation and consequently both anomers were found in the single-crystal structure.

Apparently, the NAG–lysozyme complex did not form under rapid precipitation from 0.5 *M* NaCl buffer pH 5.0 despite the more than 30-fold excess of NAG in the preparation. Careful examination of a ΔF map prepared in the same way as the pH 6.0 material show no extended density anywhere; only scattered peaks probably arising from bound water molecules were observed. Additionally, the refined lysozyme structures for the two pH 5.0 samples, one prepared with NAG and the other without, were virtually identical; the RMS distance between the two sets of backbone atoms was only 0.17 Å. In comparison, the RMS distance between the backbone atoms of the pH 6.0 materials prepared with and without NAG was 0.52 Å, indicating a change in the protein structure with complex formation. The lysozyme structure is quite pH dependent; the RMS distance between the backbone atoms of the uncomplexed pH 5.0 and pH 6.0 materials is 0.98 Å. Evidently, this structural change with pH is sufficient to prevent NAG binding under the conditions of rapid precipitation at lower pH. The effect is quite subtle, as careful residue-by-residue comparison of these moderate (∼3 Å) powder diffraction structures did not show an obvious structural change that would inhibit NAG binding to the protein prepared from pH 5.0 buffer.

Clearly, as we had observed earlier for metmyoglobin (Von Dreele, 1999) and T_3R_3 Zn insulin (Von Dreele *et al.*, 2000), polycrystalline lysozyme and NAG–lysozyme powders, prepared in this case by rapid precipitation, consist of essentially defect-free crystallites that are a few micrometres across. As noted by us earlier, these dimensions suggest that the crystallites are only a few hundred protein unit cells in extent which, when coupled with the relatively weak binding between adjacent molecules, is insufficient to retain point and line defects at ambient temperature. Consequently, powder diffraction patterns of these materials give diffraction peaks that are as sharp as can be obtained from a given diffraction instrument; this may be a common feature of ambient temperature protein powder diffraction patterns. In essence, proteins are 'perfect' powders for diffraction. In the work described here, the extreme sharpness of these patterns arose from the uniform and easily controlled precipitation conditions and allowed easy discernment of the small structural changes associated with protein–ligand complex formation and ready discrimination from cases where no complex is formed. Moreover, the quality of the powder diffraction pattern was sufficient to determine the detailed structural features of the protein–ligand complex. Thus, it is likely that high-resolution powder diffraction can facilitate both the screening for protein–ligand interactions and the determination of their resulting structures under a wide variety of conditions.[1]

[1] Supplementary data relating to this powder diffraction study are available from the IUCr electronic archive (Reference: en0052). Details on how to access these data are available at the back of the journal.

The author thanks P. Stephens and S. Pagola for assistance in collecting the powder diffraction data. The US DOE/BES under contract W-7405-ENG-36 supported this work and the SUNY X3 beamline is supported by US DOE Grant No. DE-FG02-86ER45231.

References

Aldhous, P. (2000). *Nature (London)*, **408**, 894–896.
Blake, C. C. F., Fenn, R. H., North, A. C. T., Phillips, D. C. & Poijak, R. J. (1962). *Nature (London)*, **196**, 1173–1176.
Blake, C. C. F., Johnson, L. N., Mair, G. A., North, A. C. T., Phillips, D. C. & Sarma, V. R. (1967). *Proc. R. Soc. London B*, **167**, 378–388.
Blake, C. C. F., Koenig, D. F., Mair, G. A., North, A. C. T., Phillips, D. C. & Sarma, V. R. (1965). *Nature (London)*, **206**, 757–761.
Bonincontro, A., De Francesco, A. & Onori, G. (1998). *Colloid Surf. B*, **12**, 1–5.
Cheetham, J. C., Artymiuk, P. J. & Phillips, D. C. (1992). *J. Mol. Biol.* **224**, 613–628.
Corey, R. B., Stanford, R. H. Jr, Marsh, R. E., Leung, Y. C. & Kay, L. M. (1962). *Acta Cryst.* **15**, 1157–1163.
Engh, R. A. & Huber, R. (1991). *Acta Cryst.* A**47**, 392–400.
Fong, K., Jefferson, T., Suyehiro, T. & Walton L. (1993). *Guide to the SLATEC Common Mathematical Library*. http://www.netlib.org/slatec.
Guex, N. & Peitsch, M. C. (1999). *Swiss-PdbViewer*, Glaxo Wellcome Experimental Research. http://www.expasy.ch/spdbv.
International Human Genome Sequencing Consortium (2001). *Nature (London)*, **409**, 860–921.
Johnson, L. N. & Phillips, D. C. (1965). *Nature (London)*, **206**, 761–763.
Larson, A. C. & Von Dreele, R. B. (1986). *General Structure Analysis System (GSAS)*, Los Alamos National Laboratory Report LAUR 86-748. ftp://ftp.lanl.gov/public/gsas.
Laskowski, R. A., MacArthur, M. W., Moss, D. S. & Thornton, J. M. (1993). *J. Appl. Cryst.* **26**, 283–291.
Morris, A. L., MacArthur, M. W., Hutchinson, E. G. & Thornton, J. M. (1992). *Proteins*, **12**, 345–364.
Motoshima, H., Mine, S., Masumoto, K., Abe, Y., Iwashita, H., Hasimoto, Y., Chijiiwa, Y., Ueda, T. & Imoto, T. (1997). *J. Biochem.* **121**, 1076–1081.
Pennisi, E. (2000). *Science*, **288**, 2304–2307.
Perkins, S. J., Johnson, L. N., Machin, P. A. & Phillips, D. C. (1978). *Biochem. J.* **173**, 607–616.
Perkins, S. J., Johnson, L. N., Phillips, D. C. & Dwek, R. A. (1981). *Biochem. J.* **193**, 553–572.
Phillips, D. C. (1967). *Proc. Natl Acad. Sci. USA*, **57**, 484–495.
Rietveld, H. M. (1969). *J. Appl. Cryst.* **2**, 65–71.
Rosenbaum, D. F. & Zukoski, C. F. (1996). *J. Cryst. Growth*, **169**, 752–758.
Rupley, J. A. & Gates, V. (1967). *Proc. Natl Acad. Sci.* **57**, 496–510.
Venter, J. C. *et al.* (2001). *Science*, **291**, 1304–1351.
Von Dreele, R. B. (1999). *J. Appl. Cryst.* **32**, 1084–1089.
Von Dreele, R. B., Stephens, P. W., Blessing, R. H. & Smith, G. D. (2000). *Acta Cryst.* D**56**, 1549–1553.